

Comparative Evaluation of Multiple-Model Kalman Filters for Highly Maneuvering UAV Tracking

Original

Comparative Evaluation of Multiple-Model Kalman Filters for Highly Maneuvering UAV Tracking / Lizzio, Fausto Francesco; Trombetta, Enza Incoronata; Capello, Elisa; Fujisaki, Yasumasa. - In: APPLIED SCIENCES. - ISSN 2076-3417. - ELETTRONICO. - 16:5(2026). [10.3390/app16052377]

Availability:

This version is available at: 11583/3008908 since: 2026-03-19T09:07:23Z

Publisher:

MDPI

Published

DOI:10.3390/app16052377

Terms of use:

This article is made available under terms and conditions as specified in the corresponding bibliographic description in the repository

Publisher copyright

(Article begins on next page)



Article

Comparative Evaluation of Multiple-Model Kalman Filters for Highly Maneuvering UAV Tracking

Fausto Francesco Lizzio ¹, Enza Incoronata Trombetta ¹, Elisa Capello ^{1,*} and Yasumasa Fujisaki ²

¹ Department of Aerospace and Mechanical Engineering, Politecnico di Torino, 10129 Turin, Italy; fausto.lizzio@polito.it (F.F.L.); enza.trombetta@polito.it (E.I.T.)

² Department of Information and Physical Sciences, The University of Osaka, Suita 565-0871, Osaka, Japan; fujisaki@ist.osaka-u.ac.jp

* Correspondence: elisa.capello@polito.it

Featured Application

This paper compares several Multiple-Model Kalman Filter (MMKF) approaches for tracking highly maneuvering, non-cooperative targets, focusing on how different treatments of the transition probability matrix (fixed, adaptive, or absent) affect performance. Using extensive Monte Carlo simulations, it evaluates each filter's estimation accuracy and mode identification capability, revealing key trade-offs in robustness, stability, and tracking precision.

Abstract

Tracking highly maneuvering, non-cooperative UAVs poses significant challenges due to rapid and unpredictable changes in target dynamics. Under such conditions, traditional single-model filters often fail to maintain reliable state estimates, resulting in degraded tracking performance. Multiple-Model Kalman Filter (MMKF) approaches, including the Generalized Pseudo Bayesian (GPB1) and Interacting Multiple-Model (IMM) algorithms, improve robustness by simultaneously considering multiple candidate motion models and weighting them according to the observed target behavior. Adaptive strategies, such as χ^2 -test-based or t -test-based methods, further enhance performance by dynamically responding to changes in maneuvering patterns. This paper presents a multi-criteria comparative assessment of four MMKF formulations—GPB1, IMM, χ^2 -test-based, and t -test-based filters—under a consistent modeling and simulation framework. Particular emphasis is placed on systematically analyzing the role of the transition probability matrix (TPM), investigating how fixed, adaptive, and TPM-free strategies affect estimation accuracy, robustness to noise, and mode-identification performance. Beyond conventional Root Mean Square Error (RMSE) metrics, the filters' comparison is carried out through confusion matrices and dwell time analysis to highlight performance nuances and trade-offs. This allows to establish which filter formulation is preferable in different operational conditions.



Academic Editors: Xiaoping Xu, Rui Wang and Rosario Pecora

Received: 15 January 2026

Revised: 20 February 2026

Accepted: 25 February 2026

Published: 28 February 2026

Copyright: © 2026 by the authors.

Licensee MDPI, Basel, Switzerland.

This article is an open access article distributed under the terms and conditions of the [Creative Commons Attribution \(CC BY\) license](https://creativecommons.org/licenses/by/4.0/).

Keywords: multiple-model Kalman filter; interacting multiple models; non-collaborative target tracking; Monte Carlo simulations

1. Introduction

Accurate state estimation is crucial for tracking highly maneuvering, non-cooperative targets, as it provides the critical information needed to predict future motion and enable timely decision-making. Modern UAVs can execute rapid and unpredictable maneuvers, often switching between different flight modes, such as steady flight, acceleration, or sharp

turns. These dynamic behaviors make it difficult for traditional single-model filters, which assume a fixed motion model, to maintain accurate state estimates [1]. Even small errors in position or velocity estimation can propagate rapidly, degrading tracking performance and potentially compromising mission objectives. Therefore, reliable UAV tracking is essential for safe navigation, collision avoidance, mission planning, autonomous control, and situational awareness in complex environments.

In the literature, Kalman filters (KFs) have been widely adopted for target tracking, with numerous extensions proposed to address practical challenges, such as nonlinear process and measurement models—commonly handled using the Extended or Unscented Kalman filters (EKF/UKF) [2]—as well as decentralized estimation architectures, which have motivated the development of Information KFs [3,4]. However, in UAV tracking applications, target dynamics can evolve rapidly and switch between distinct motion patterns, making it difficult to maintain accurate state estimates using a single fixed motion model. Multiple-model approaches, such as the Multiple-Model Kalman Filter (MMKF) [5], address these challenges by simultaneously considering several possible motion models and dynamically weighting them according to the observed UAV behavior, improving robustness and accuracy across varying flight regimes [6]. By explicitly representing motion uncertainty through a set of candidate dynamic models, multiple-model filtering frameworks generally achieve superior estimation performance under such conditions.

Among these approaches, the Generalized Pseudo Bayesian and the Interacting Multiple-Model algorithms have emerged as effective and computationally efficient solutions. The First-Order Generalized Pseudo Bayesian (GPB1) algorithm executes several model-conditioned prediction and update steps in parallel, followed by a fusion stage that combines the resulting state estimates and covariances into a single composite estimate, weighted according to their respective mode probabilities [7]. The *Interacting Multiple-Model* (IMM) algorithm extends this framework by introducing an additional mixing step, whereby each model's initial condition at the subsequent time step is computed as a weighted combination of all model-conditioned estimates from the previous step, using the mode transition probabilities [8]. Both algorithms rely on a transition probability matrix (TPM) to represent the likelihood of switching between motion models at each time step. Typically, the TPM is fixed with high diagonal entries, reflecting the assumption that the UAV will remain in the same maneuvering mode over consecutive steps. In practice, however, the true mode sequence is unknown and depends critically on unknown control inputs; moreover, it may not strictly follow a Markov process. Consequently, the design or tuning of the TPM aims to select a Markov transition law that “best” approximates the unknown target behavior, similarly to the tuning of the process noise covariance Q in Kalman filtering. While estimation performance is generally not highly sensitive to the exact TPM choice, provided it is not severely mismatched, the TPM nevertheless introduces an important trade-off between peak estimation errors at maneuver onset and termination and steady-state errors during constant-velocity motion [9]. To account for the highly dynamic and unpredictable behavior of real UAVs, adaptive approaches have been developed to update the transition probabilities online, improving overall estimation performance [10–12]. More recent approaches have explored strategies that (i) integrate into the IMM framework a χ^2 -test to adjust the TPM parameters dynamically based on the observed target motion [13], or (ii) avoid the explicit use of a TPM while still operating within an MMKF framework. In [14], a t -test procedure is proposed, in which the algorithm evaluates the most recent samples of the innovation vectors from each model and selects the estimate with the lowest t -value. Unlike the other strategies, each model maintains its own state estimate and covariance for the next iteration, and the models are not combined into a single composite estimate.

Due to differences in their underlying assumptions, model interaction schemes, and prior knowledge of the target, the MMKF formulations discussed above can exhibit varying performance under different operational conditions. In this paper, we present a comparative assessment of four MMKF approaches—GPB1, IMM, χ^2 -test-based, and t -test-based filters—specifically for tracking the state of a highly maneuvering UAV. The study is intended as a conceptual investigation to assess the comparative performance of these MMKF approaches, rather than to provide a full-scale implementation for operational UAVs. A Monte Carlo simulation framework is developed to evaluate the performance of these algorithms across a diverse set of UAV trajectories. The study aims to quantify relative estimation performance in terms of Root Mean Square Error (RMSE), mode probability accuracy, and dwell time.

The main contributions of this study can be summarized as follows:

1. A unified comparison of four MMKF formulations (GPB1, IMM, χ^2 -test-based, and t -test-based filters) under a consistent modeling and simulation framework.
2. A systematic assessment of the role of the transition probability matrix (TPM), analyzing how fixed, adaptive, or TPM-free approaches influence estimation accuracy, robustness, and mode identification performance.
3. A Monte Carlo evaluation across 100 randomly generated maneuvering trajectories to ensure statistically meaningful performance comparisons.
4. A performance analysis that goes beyond classical RMSE metrics by incorporating confusion matrices and dwell time as indicators of model-identification capability.

This paper is organized as follows. Section 2 provides some preliminaries on MMKF, while Section 3 describes the selected MMKF formulations to be compared. The simulation environment and the numerical results are presented in Section 4, together with several considerations on filters' performance. Finally, some concluding remarks, along with a comment on future works, are reported in Section 5.

2. Preliminaries

Reliable target tracking requires precise motion representation and effective extraction of state information from sensor observations [15]. To capture the varying dynamic behaviors of a target more effectively, multiple mathematical models are employed, providing a richer and more flexible characterization of its motion. In the following, we introduce the system modeling framework, outline the estimation methods for inferring the target state from observations, and describe strategies for fusing estimates from multiple models to enhance overall state estimation performance.

2.1. Modeling the Target Motion

Although a target is rarely a true point in space and its orientation can provide valuable information for tracking, it is typically modeled as a point object without explicit shape, with the primary goal of estimating its position and velocity over time.

Almost all types of target motion can be described by the following discrete state-space model:

$$x_k = f_{k-1}(x_{k-1}, u_{k-1}, w_{k-1}), \quad (1)$$

where x is the state vector, u is the control input, k the time index and w the process noise. The control input is typically unknown to the tracker and can be handled (i) as an unknown deterministic process, which can be estimated from measurement data during tracking, or (ii) as a random process, where the effect of maneuvers is represented by a white (or colored) noise process. The latter approach is adopted.

In this paper, the evolution of the target state is assumed to be well described by a *jump Markovian system*, in which transitions between r system models are governed by a transition probability matrix $\Pi_k \in \mathbb{R}^{r \times r}$. The elements $\pi_{ij,k}$ of Π_k represent the probability that the system transitions from mode i at time $k - 1$ to mode j at time k . The r models correspond to the possible candidates for the true mode active at a given time k , where a *mode* represents a characteristic pattern of system behavior [9]. The mode probability $\mu_{i,k}$ represents the likelihood that model i corresponds to the true mode at time k .

The i th model for the target dynamics, with $i = 1, \dots, r$, obeys

$$\begin{aligned} x_{i,k} &= A_{i,k-1} x_{i,k-1} + w_{i,k-1}, \\ z_k &= H_{i,k} x_{i,k} + v_k, \end{aligned} \tag{2}$$

where $x_{i,k} \in \mathbb{R}^{n_i}$ is the state vector of dimension n_i , $A_{i,k-1} \in \mathbb{R}^{n_i \times n_i}$ the state transition matrix, $z_k \in \mathbb{R}^p$ the measurement vector of dimension p , $H_{i,k} \in \mathbb{R}^{p \times n_i}$ the observation matrix, $w_{i,k} \in \mathbb{R}^{n_i}$ the input white noise with covariance matrix $Q_{i,k-1} \in \mathbb{R}^{n_i \times n_i}$, and $v_k \in \mathbb{R}^p$ the measurement white noise with covariance matrix $R_k \in \mathbb{R}^{p \times p}$.

Common motion models include *constant acceleration* (CA), *constant velocity* (CV), and *constant turn* (CT) [15], which respectively describe motion with uniform velocity, motion with steady acceleration, and coordinated turning at a constant turn rate. These are the most common choices for airborne vehicles, as their combined use can handle most of the expected maneuvers, [16,17].

2.2. Estimating the Target Motion

Consider r separate Kalman filters running in parallel, where the dynamics of filter i is defined by the model i in (2). Let $\hat{x}_{i,k|k-1} \in \mathbb{R}^{n_i}$ and $P_{i,k|k-1} \in \mathbb{R}^{n_i \times n_i}$ denote the predicted state and covariance matrix associated with model i . Similarly, let $\hat{x}_{i,k|k} \in \mathbb{R}^{n_i}$ and $P_{i,k|k} \in \mathbb{R}^{n_i \times n_i}$ denote the updated (estimated) state and covariance for model i .

The initial estimates $\hat{x}_{i,0|0}$ and $P_{i,0|0}$ are set based on a priori knowledge of the process and initialized consistently for all filters, with dimensions tailored to each filter’s state vector. The prediction step of filter i at time step k is given by

$$\begin{aligned} \hat{x}_{i,k|k-1} &= A_{i,k-1} \hat{x}_{i,k-1|k-1}, \\ P_{i,k|k-1} &= A_{i,k-1} P_{i,k-1|k-1} A_{i,k-1}^T + Q_{i,k-1}, \end{aligned} \tag{3}$$

while the update step is given by

$$\begin{aligned} \hat{x}_{i,k|k} &= \hat{x}_{i,k|k-1} + K_{i,k} v_{i,k}, \\ P_{i,k|k} &= (I_{n_i} - K_{i,k} H_{i,k}) P_{i,k|k-1}, \end{aligned} \tag{4}$$

where

$$\begin{aligned} K_{i,k} &= P_{i,k|k-1} H_{i,k}^T S_{i,k}^{-1}, \\ v_{i,k} &= z_k - H_{i,k} \hat{x}_{i,k|k-1}, \\ S_{i,k} &= H_{i,k} P_{i,k|k-1} H_{i,k}^T + R_k. \end{aligned} \tag{5}$$

are the Kalman gain, the innovation at time k of mode i , and the innovation covariance, respectively.

A generic multiple-model algorithm aims to obtain an overall state estimate $\hat{x}_{k|k}$ and covariance $P_{k|k}$ for the system as weighted combination of the estimates $\hat{x}_{i,k|k}$ and covariances $P_{i,k|k}$ from the individual filters.

Figure 1 conceptually summarizes the processing pipeline: (i) r motion models are run in parallel to capture different target dynamics; model-conditioned predictions are generated, and each filter updates its state estimate by computing the innovation and evaluating the likelihood of the measurements under its model; (ii) depending on the fusion strategy, estimates are fused, mixed, or the most probable model is selected; finally, (iii) a global state estimate is produced by combining information from all models.

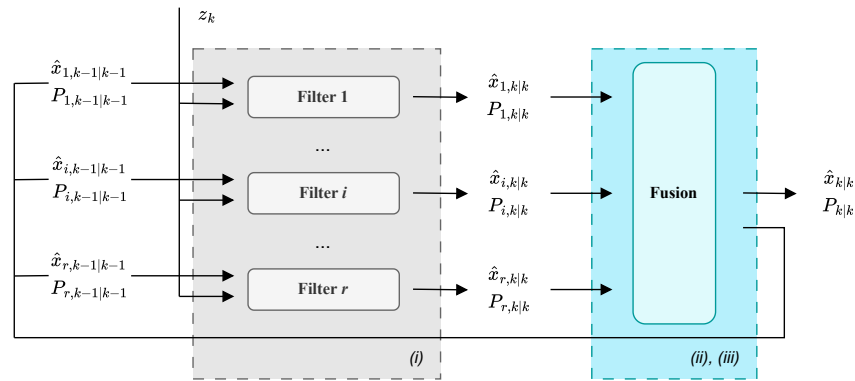


Figure 1. Processing pipeline for multi-model state estimation.

A centralized processing architecture is adopted, in which measurements from all sensors are collected and jointly processed by all filters. To allow for the fusion of estimates, an augmentation/truncation procedure is required to align the state and covariance dimensions among the different filters. If the state vector estimated by filter i has fewer components than that of filter j , the common states are retained, and the state vector and covariance matrix are truncated by removing all elements corresponding to the states not estimated by filter i . Conversely, if filter i has more components than filter j , the state vector and covariance are augmented and aligned according to the unbiased transformation procedure described in [18].

2.3. Fusing the Estimates

In multi-model filtering frameworks, each filter produces a state estimate and an associated covariance matrix, which must be combined to obtain a single global state for accurate tracking of maneuvering targets. This combination can be achieved through different strategies. Fusion-based approaches integrate all model estimates into a global estimate using a weighted average based on mode probabilities, as in the GPB1 and IMM filters. The mixing strategy in the IMM filter goes further by probabilistically combining the model states before the prediction step, using mode probabilities to generate mixed initial conditions for each filter. Alternatively, statistical hypothesis-based methods, including χ^2 -test and t -test filters, monitor innovations to detect maneuvers and adapt the filter estimate accordingly.

A key element in multi-model fusion is the specification of the transition probability matrix (TPM), which encodes the assumed Markovian switching behavior between motion models. Traditionally, the TPM has been treated as an a priori design parameter, motivated by the observation that multi-model estimation performance is often relatively insensitive to the exact TPM choice, provided it is not severely mismatched [9]. Nevertheless, inappropriate TPM settings can lead to increased peak estimation errors, degraded mode identification, and lead to misleading state estimates [13]. Since this offline design is entirely a priori, it does not exploit information available from online measurements. To overcome these limitations, a number of approaches have been proposed to estimate or adapt the TPM online, while alternative methods avoid explicit TPM specification altogether. As

shown in Section 4, these differing treatments of the TPM influence estimation accuracy, robustness, and mode identification performance.

3. Multiple-Model Filtering

The *Fusion* block illustrated in Figure 1 is examined in this section for four representative algorithms, namely the GPB1, IMM, χ^2 -test-based, and *t*-test-based filters. In particular, the formulation of each algorithm is analyzed, along with the role of the TPM, the procedure used to obtain the global state estimate, and any filter reinitialization mechanisms involved.

3.1. First-Order Generalized Pseudo Bayesian Filter

The GPB1 filter operates by running *r* mode-matched Kalman filters in parallel, all driven by the same set of measurements. Starting from a global state estimate $\hat{x}_{k-1|k-1}$ and its covariance $P_{k-1|k-1}$, each filter *i* produce its own estimate $\hat{x}_{i,k|k}$ and covariance $P_{i,k|k}$ through the prediction and update steps defined in (3) and (4).

For each filter, the predicted mode probability is computed as

$$\mu_{i,k|k-1} = \sum_{j=1}^r \pi_{ji} \mu_{j,k-1|k-1}, \tag{6}$$

The likelihood of mode *i* given the measurement at time *k* is evaluated as

$$\Lambda_{i,k} = \frac{\exp(-\frac{1}{2} v_{i,k}^T S_{i,k}^{-1} v_{i,k})}{\sqrt{|(2\pi)^p S_{i,k}|}}, \tag{7}$$

with $v_{i,k}$ and $S_{i,k}$ the innovation and the corresponding covariance, defined in (5). The predicted mode probabilities $\mu_{i,k|k-1}$ are then updated using the measurement likelihoods according to

$$\mu_{i,k|k} = \frac{\Lambda_{i,k} \mu_{i,k|k-1}}{\sum_{j=1}^r \Lambda_{j,k} \mu_{j,k|k-1}}. \tag{8}$$

Finally, a fusion step is performed in which the overall state estimate and covariance are obtained as weighted combinations of the model-conditioned estimates and covariances:

$$\begin{aligned} \hat{x}_{k|k} &= \sum_{i=1}^r \mu_{i,k|k} \hat{x}_{i,k|k}, \\ P_{k|k} &= \sum_{i=1}^r \mu_{i,k|k} [P_{i,k|k} + (\hat{x}_{i,k|k} - \hat{x}_{k|k})(\hat{x}_{i,k|k} - \hat{x}_{k|k})^T]. \end{aligned} \tag{9}$$

Note that each of the *r* models starts the next filtering iteration at time *k* + 1 using the same overall state estimate and covariance obtained from step *k*.

3.2. Interacting Multiple Model Filter

The IMM extends the GPB1 approach by introducing an additional *mixing step*, also referred to as the *interaction step*, in which the model-conditioned estimates are combined according to the mode transition probabilities and used to initialize each filter. Specifically, before the prediction phase, each model *i* computes its *mixed initial condition* as a probabilistic combination of the previous model-conditioned estimates:

$$\begin{aligned} \hat{x}_{i,k-1|k-1}^0 &= \sum_{j=1}^r \mu_{j|i,k-1} \hat{x}_{j,k-1|k-1}, \\ P_{i,k-1}^0 &= \sum_{j=1}^r \mu_{j|i,k-1} [P_{j,k-1|k-1} + (\hat{x}_{j,k-1|k-1} - \hat{x}_{i,k-1|k-1}^0)(\hat{x}_{j,k-1|k-1} - \hat{x}_{i,k-1|k-1}^0)^T], \end{aligned} \tag{10}$$

where $\mu_{j|i,k-1}$ denotes the *mixing probability*, i.e., the probability that the system was in mode i at time $k - 1$ given that it is in mode j at time k . We compute the mixing probability $\mu_{i|j,k-1}$ as

$$\mu_{i|j,k-1} = \frac{\pi_{ij} \mu_{i,k-1}}{\sum_{\ell=1}^r \pi_{\ell j} \mu_{\ell,k-1}}. \tag{11}$$

Each model i then performs its standard prediction step starting from the mixed initial conditions. The combination of model-conditioned estimates and covariances follows the same weighted fusion rule used in the GPB1. Owing to the interaction step, the IMM formulation typically yields smoother transitions between modes and improved estimation performance compared to GPB1, while maintaining significantly lower computational complexity than higher-order Generalized Pseudo Bayesian filters. In this paper, we employ the IMM formulation described in [19].

3.3. χ^2 -Test-Based Filter

When tracking non-cooperative or highly maneuvering targets, the use of a fixed TPM may result in poor mode adaptation and degraded tracking performance. To address this limitation, an adaptive strategy based on the χ^2 statistical test can be employed to adjust Π_k online according to the updated model probabilities [13].

To capture the evolution of model transitions, a set of transition counters $n_{ij,k}$ is updated online. Specifically, the counter corresponding to the transition from model i to model j is incremented at time step k if model i is the most probable model at time step $k - 1$ and model j is identified as the most probable model at time step k . This mechanism enables the online monitoring of observed mode switches between consecutive time steps. Denote as

$$n_{i,k} = \sum_{j=1}^r n_{ij,k} \tag{12}$$

the total number of transitions from model i at time k . Using the retention model framework, the candidate time-varying TPM Π_k is expressed through the retention decomposition as

$$\Pi_k = D_k + (I - D_k)M_k, \tag{13}$$

where D_k and M_k are two auxiliary matrices, whose elements are defined as

$$\begin{cases} d_{ii,k} = \frac{n_{ii,k}}{n_{i,k}}, & i = 1, \dots, r, \\ d_{ij,k} = 0, & i \neq j, \end{cases} \tag{14}$$

and

$$\begin{cases} m_{ii,k} = 0, & i = 1, \dots, r, \\ m_{ij,k} = \frac{n_{ij,k}}{n_{i,k} - n_{ii,k}}, & i \neq j, \end{cases} \tag{15}$$

respectively. To determine how Π_k should be updated, four nested hypotheses are tested:

$$\begin{aligned}
 H_0 : \Pi_k^{(0)} &= D_{k-1} + (I - D_{k-1})M_{k-1}, \\
 H_1 : \Pi_k^{(1)} &= D_k + (I - D_k)M_{k-1}, \\
 H_2 : \Pi_k^{(2)} &= D_{k-1} + (I - D_{k-1})M_k, \\
 H_3 : \Pi_k^{(3)} &= D_k + (I - D_k)M_k.
 \end{aligned} \tag{16}$$

Specifically, H_0 corresponds to a stationary behavior, in which the target exhibits a consistent maneuvering pattern, and no update of the TPM is required. The hypothesis H_1 captures a change in switching frequency, indicating that the target alters modes more or less frequently, while the overall pattern of transitions remains similar. Under H_2 , the switching structure itself changes: the target maintains the same overall switching frequency, but transitions occur to different modes. Finally, H_3 represents fully non-stationary behavior, in which both the frequency and the nature of mode transitions vary over time. Let $n_{DOF} = k \cdot r \cdot (r - 1)$ denote the degrees of freedom, corresponding to the number of independent TPM parameters tested over successive time steps $k = 1, \dots, T$. A significance threshold is set as $\eta = \chi^2(0.95, n_{DOF})$, and a standard χ^2 -test statistic is applied to determine the hypothesis that best fits the current observations. Once a hypothesis is selected, the corresponding transition probability matrix, Π_k , is used to update the filters. The active model at time k is selected as the one with the highest posterior probability, i.e.,

$$i_k^* = \arg \max_i \mu_{i,k|k} \tag{17}$$

where $\mu_{i,k|k}$ denotes the posterior probability of model i , computed according to the standard IMM updating procedure.

3.4. *t*-Test-Based Filter

In the *t*-test formulation, model-conditioned estimates are fused directly based on statistical consistency, eliminating the need for a TPM while maintaining a formulation consistent with the MMKF framework [14]. The estimator identifies the model that provides the most statistically consistent estimate with the current measurement. Statistical consistency is assessed by comparing the magnitudes of the normalized innovations for each model. To enhance robustness and mitigate the effect of measurement noise, the innovations are accumulated over a fixed window of n_s samples.

For each model i , the stored innovations are used to compute the average innovation magnitude:

$$\bar{v}_{i,k} = \frac{1}{n_s} \sum_{t=k-n_s+1}^k v_{i,t}, \tag{18}$$

and the corresponding covariance estimate

$$\bar{S}_{i,k} = \frac{1}{n_s} \sum_{t=k-n_s+1}^k S_{i,t}. \tag{19}$$

The *t*-test is then employed to assess whether the mean innovation of each model differs significantly from zero. The test statistic for model i is given by

$$T_{i,k} = \frac{\|\bar{v}_{i,k}\|}{\sqrt{\text{trace}(\bar{S}_{i,k})/n_s}}, \tag{20}$$

which normalizes the average innovation by its expected dispersion over the observation window. The model producing the smallest $T_{i,k}$ value is considered the most consistent with the current measurement, and it is selected as the active model at time k :

$$i_k^* = \arg \min_i T_{i,k}. \tag{21}$$

It should be noted that the r models operate independently, and no fusion procedure is applied. The value n_s must represent a trade-off between robustness to measurement noise, memory requirements, and the responsiveness of the test.

4. Simulation and Results

This section presents a comparative analysis of the tracking performance achieved by the four MMKF approaches for UAV tracking, with particular emphasis on assessing how the TPM influences estimation accuracy and mode identification capability. The following subsections describe the simulation setup and scenario, outline the performance metrics used for evaluation, and present the simulation results, highlighting the relative strengths and limitations of each filtering approach under different TPM or parameter configurations.

4.1. Simulation Settings

The evaluation is conducted through Monte Carlo simulations implemented in the MATLAB 2025b/Simulink environment. A total of 100 target trajectories is generated to represent the motion of the UAV. Each trajectory has a duration of $T = 500$ s, divided into fifteen intervals with lengths determined randomly. For each interval, the active target motion model is selected by sampling from a uniform discrete distribution over $\{1, 2, 3\}$, corresponding to the *Constant Acceleration* (CA), *Constant Velocity* (CV), and *Constant Turn* (CT) models, chosen for their representativeness of the UAV motion [15]. The sampling procedure ensures that every motion model is applied at least once within each trajectory. Specifications of the models are as follows:

- CA: accelerations are chosen from a Gaussian distribution whose mean is 5 m/s^2 and whose standard deviation is 1 m/s^2 .
- CV: the target keeps the same velocity it reached during the previous phase. If it is the first phase, it maintains an initial velocity of 0.5 m/s along both axes.
- CT: the turning rate is selected from a uniform distribution whose minimum is -20 deg/s and whose maximum is 20 deg/s .

We establish these parameter settings based on characteristics of target motion reported in the literature. In particular, the selected values correspond to typical ranges used to model highly maneuvering targets. A similar test-bed is adopted in [14,20]. The sampling time of the estimation process is $\Delta T = 1$ s (the sampling frequency is 1 Hz). This sampling value is such that consecutive state variations are sufficiently pronounced to make the dynamic differences among the adopted motion models clearly distinguishable, whereas a significantly higher sampling frequency would reduce inter-sample variability and diminish model separability.

The filters are initialized with $\hat{x}_{i,0|0} = 0_{n_i \times 1}$ and $P_{i,0|0} = I_{n_i}$, for $i = 1, 2, 3$. The process noise covariance matrix is constant and given by

$$Q_{CV} = \begin{bmatrix} \frac{1}{2}\Delta T^2 & 0 & 0 & 0 \\ 0 & \Delta T & 0 & 0 \\ 0 & 0 & \frac{1}{2}\Delta T^2 & 0 \\ 0 & 0 & 0 & \Delta T \end{bmatrix}$$

for a state vector $[x, \dot{x}, y, \dot{y}]$,

$$Q_{CT} = \begin{bmatrix} \frac{1}{2}\Delta T^2 & 0 & 0 & 0 & 0 \\ 0 & \Delta T & 0 & 0 & 0 \\ 0 & 0 & \frac{1}{2}\Delta T^2 & 0 & 0 \\ 0 & 0 & 0 & \Delta T & 0 \\ 0 & 0 & 0 & 0 & \Delta T \end{bmatrix},$$

for a state vector $[x, \dot{x}, y, \dot{y}, \omega]$,

$$Q_{CA} = \begin{bmatrix} \frac{1}{2}\Delta T^2 & 0 & 0 & 0 & 0 & 0 \\ 0 & \Delta T & 0 & 0 & 0 & 0 \\ 0 & 0 & 1 & 0 & 0 & 0 \\ 0 & 0 & 0 & \frac{1}{2}\Delta T^2 & 0 & 0 \\ 0 & 0 & 0 & 0 & \Delta T & 0 \\ 0 & 0 & 0 & 0 & 0 & 1 \end{bmatrix}.$$

for a state vector $[x, \dot{x}, \ddot{x}, y, \dot{y}, \ddot{y}]$. The measurement consists of the absolute position of the target in the X-Y inertial reference frame expressed in m , while the noise covariance is also considered constant and equal to

$$R_k = \begin{bmatrix} R_X & 0 \\ 0 & R_Y \end{bmatrix}.$$

with $R_X, R_Y = 2 \text{ m}^2$. The GPB1 and the IMM algorithms are tested with two versions of the TPM, i.e.,

$$\Pi_a = \begin{bmatrix} 0.90 & 0.05 & 0.05 \\ 0.05 & 0.90 & 0.05 \\ 0.05 & 0.05 & 0.90 \end{bmatrix},$$

and

$$\Pi_b = \begin{bmatrix} 0.33 & 0.33 & 0.33 \\ 0.33 & 0.33 & 0.33 \\ 0.33 & 0.33 & 0.33 \end{bmatrix}.$$

The two versions are designed to emphasize the impact of selecting a transition probability matrix that is either close to the true TPM governing the target trajectories (Π_a) or significantly different from it (Π_b). Specifically, through high self-transition probabilities, Π_a characterizes the persistence of UAV motion modes over time. In contrast, Π_b represents a deliberately uninformative benchmark case, in which all transitions are equally likely, corresponding to a complete lack of prior knowledge about the target maneuvering behavior.

The initialization of the χ^2 -test-based filter requires a set of counters $n_{ij,0} \neq 0$ to prevent numerical issues. In this work, $n_{ij,0} = 0.001$ for $i, j = 1, \dots, r$ is used to avoid introducing bias in the initial estimates. The t -test-based filter is tested by storing $n_s = 10$ previous samples of the innovation vector, as done in [14], and $n_s = 20$, to assess the effect of the accumulation window length on filter performance.

4.2. Performance Metrics

The performance of the algorithms is evaluated using classical metrics, such as the RMSEs of the estimated position and velocity with respect to the true state, as well as specific metrics designed to assess the model identification accuracy, i.e., the ability of the filter to recognize the active motion model at each time step correctly.

The *confusion matrix* is a table that shows how often the filter correctly or incorrectly identifies the actual system mode. High values along the diagonal indicate that the filter accurately detects the active model most of the time, while high off-diagonal values suggest frequent confusion between models. The *dwell time* measures the duration for which the filter remains in a given model after switching to it. A dwell time comparable to that of the actual target motion indicates that the filter maintains stability and is appropriately insensitive to measurement noise. Conversely, excessively high dwell times imply that the filter adapts too slowly to changes in the target’s motion, leading to delayed responses and increased estimation errors during transitions. Low dwell times, on the other hand, indicate frequent model switching, which may reflect overreaction to noise rather than actual maneuvering.

4.3. Results

The Monte Carlo simulation results, expressed in terms of RMSE, are summarized in Table 1. The confusion matrices are shown in Figure 2a,b for the GPB1 filter with $\text{TPM} = \Pi_a$ and $\text{TPM} = \Pi_b$, in Figure 3a,b for the IMM filter with $\text{TPM} = \Pi_a$ and $\text{TPM} = \Pi_b$, in Figure 4 for the χ^2 -test-based filter, and in Figure 5a,b for the t -test-based filter with $n_s = 10$ and $n_s = 20$, respectively. Bright colors indicate a high percentage of correct model identification, whereas darker colors correspond to lower identification accuracy. The dwell time results are reported in Figure 6.

Table 1. RMSE comparison for position and velocity components across filters.

	$x [m]$	$y [m]$	$\dot{x} [m/s]$	$\dot{y} [m/s]$
GPB1 (Π_a)	1.3032	1.3029	2.9561	2.8410
GPB1 (Π_b)	1.3148	1.3182	3.1207	3.0079
IMM (Π_a)	1.3150	1.3164	3.1000	2.9910
IMM (Π_b)	1.3823	1.3953	3.4359	3.3745
χ^2 -test	1.3306	1.3332	3.1220	3.0436
t -test (10)	1.5946	1.5385	4.2476	3.8257
t -test (20)	1.6283	1.5717	4.3225	3.8698

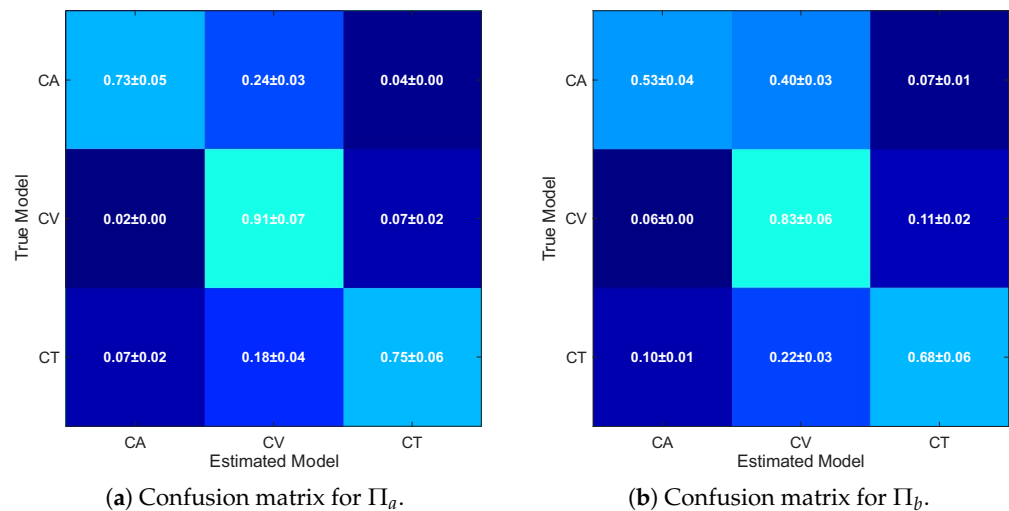


Figure 2. Comparison of confusion matrices for GPB1 filters with different TPMs.

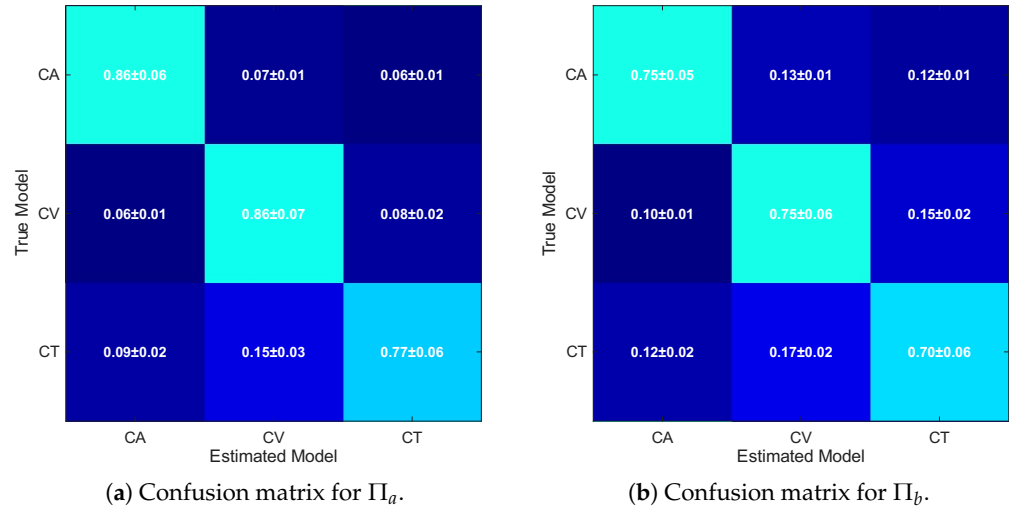


Figure 3. Comparison of confusion matrices for IMM filters with different TPMs.

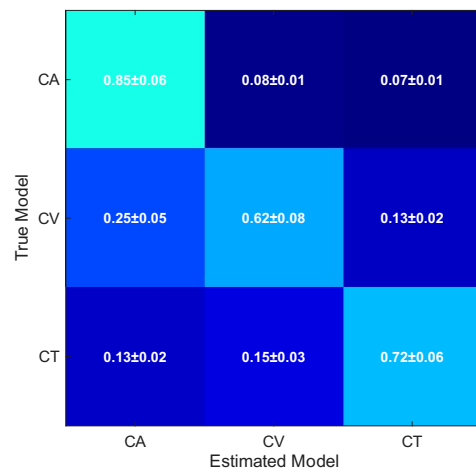


Figure 4. Confusion matrix for the χ^2 -test-based filter.

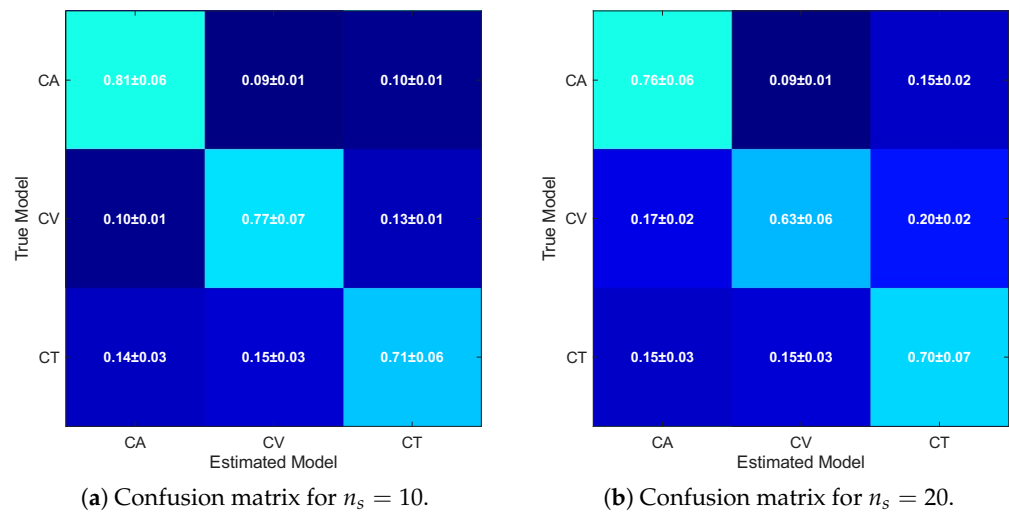


Figure 5. Comparison of confusion matrices for the t -test-based filter with different n_s .

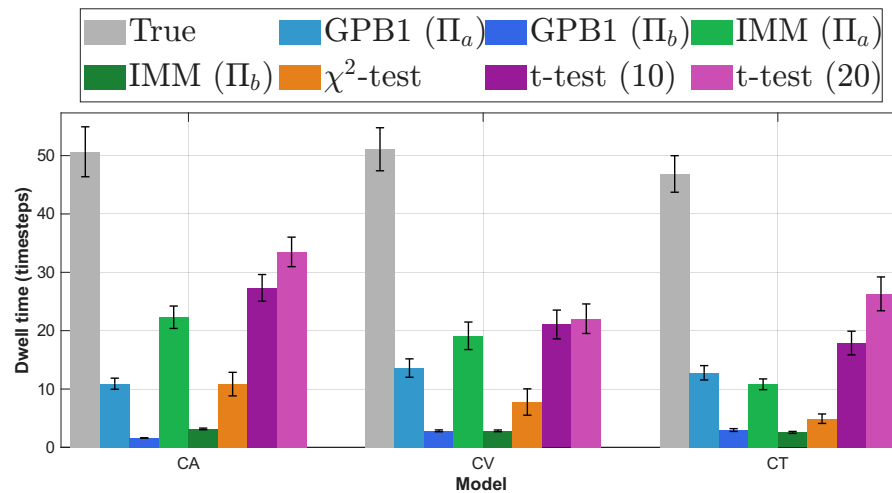


Figure 6. True vs. estimated dwell times across filters.

When using a $TPM = \Pi_a$ that is close to the actual target TPM, the GPB1 and IMM achieve the lowest RMSEs, with nearly identical results, particularly for position estimates. The IMM exhibits slightly higher RMSE in velocity compared to GPB1 but outperforms it in model identification, as reflected in the analysis of the confusion matrices and dwell times. When adopting a $TPM = \Pi_b$ significantly different from the true one, both filters experience performance degradation across all metrics. The most pronounced decline occurs for GPB1 in terms of model identification, while both filters show drastically reduced dwell times. In contrast, RMSE increases remain relatively modest, particularly for GPB1, indicating that estimation accuracy is less sensitive to TPM mismatches than mode identification and filter stability.

Adaptive strategies also perform well. The χ^2 -test-based filter closely matches GPB1 and IMM with $TPM = \Pi_a$. By analyzing the confusion matrix, we notice that the filter achieves satisfactory model identification accuracy due to its online TPM adaptation. More in detail, we see that the CA and CT models are correctly identified with high accuracy, while the CV model is recognized only, on average, the 62% of the time. Notably, CV motion is confused with CA in 25% of cases, which is reasonable since a CV trajectory can be approximated by a CA model with zero acceleration. Moreover, the χ^2 -test relies on instantaneous innovation values, making it more sensitive to measurement noise and short-term fluctuations, thereby increasing the likelihood of transient misclassification. However, the χ^2 -test-based filter exhibits relatively low dwell times, suggesting that updating counters based on the model probabilities $\mu_{i,k|k}$ can lead to overreaction to noise. Nevertheless, its dwell times remain higher than those of GPB1 and IMM when using $TPM = \Pi_b$.

Finally, the t -test-based filter shows the highest RMSEs for both position and velocity. When $n_s = 10$, the confusion matrix shows an accuracy which is higher than the one achieved by the χ^2 -test-based filter, and only slightly lower than the one achieved by GPB1 and IMM. Storing $n_s = 10$ previous innovation samples makes the method less sensitive to noise. Increasing the sample size to $n_s = 20$ further improves the dwell time, but degrades RMSE and mode identification metrics, indicating that the filter becomes too slow to respond to sudden target maneuvers.

4.4. Sensitivity Analysis

To assess the robustness of the filters to changes in measurement uncertainty, we performed a sensitivity analysis by varying the measurement noise covariance R . Specifically, we varied R_X and R_Y across values of 0.5, 1, 2, and 10 m^2 . For each configuration, the

filters were evaluated in terms of tracking accuracy (RMSE), model identification accuracy, and normalized dwell time, averaged over 10 Monte Carlo runs. Results are shown in Figures 7–9 for RMSE on position, accuracy of model identification and dwell time respectively. IMM demonstrates the highest robustness, maintaining the best classification accuracy across all noise levels and exhibiting smooth growth in both position and velocity RMSE. GPB1 follows closely at low noise but shows slightly greater sensitivity as R increases. The χ^2 -test-based methods degrade more rapidly, particularly at high noise levels, indicating stronger sensitivity to likelihood flattening. The t -test filter maintains comparatively stable accuracy at large R , though at the cost of higher RMSE. Overall, increasing measurement noise primarily affects model discrimination rather than causing catastrophic state divergence. Among the evaluated methods, IMM offers the best trade-off between robustness, estimation accuracy, and switching stability under measurement uncertainty.

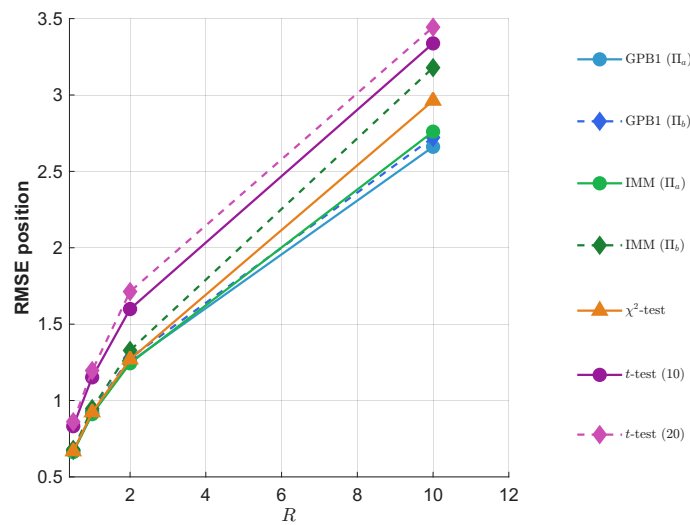


Figure 7. RMSE on position (mean of x and y components) as a function of the measurement noise covariance R . Multi-model algorithms (solid and dashed lines) are compared.

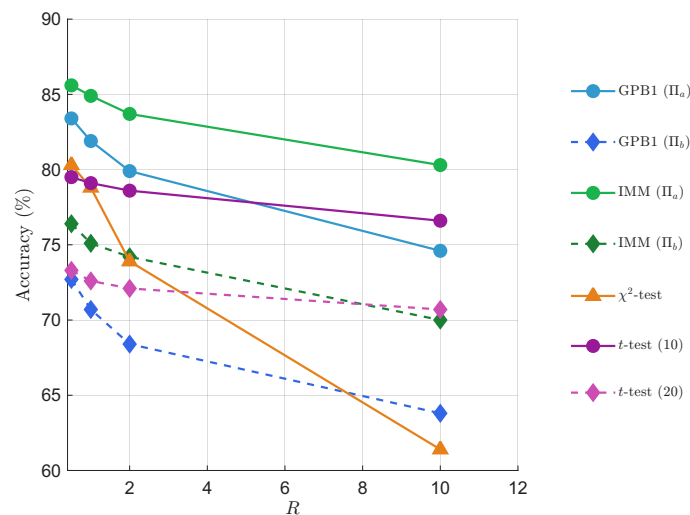


Figure 8. Model identification accuracy (%) as a function of the measurement noise covariance R .

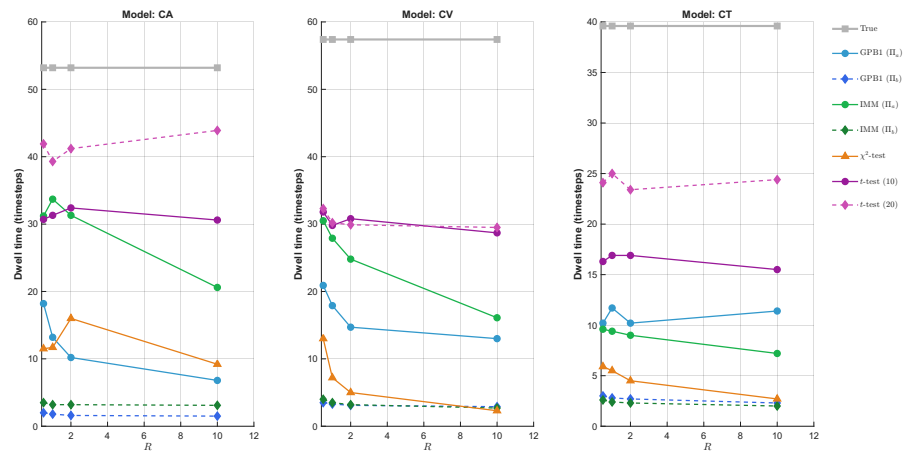


Figure 9. Estimated dwell time as a function of R for each motion model (CA, CV, CT).

4.5. Discussion

The comparative analysis highlights several key insights regarding MMKF performance for UAV tracking. The accurate choice for the transition probability matrix affects performance: filters using a TPM close to the true target transitions achieve lower RMSEs and better model identification, while deviations from the true TPM degrade confusion matrix accuracy and dwell times, even when RMSE increases remain moderate.

Adaptive strategies, such as the χ^2 -test-based filter, effectively update the TPM online, achieving performance comparable to MMKFs with an accurate prior TPM and proving particularly suitable when no a priori knowledge of the target behavior is available, although they exhibit some sensitivity to noise. The *t*-test-based filter, which does not rely on a TPM, delivers satisfactory results in terms of both confusion matrix accuracy and dwell time; however, its performance depends strongly on the size of the accumulation window, reflecting a trade-off between responsiveness and robustness.

The comparative results highlight that no single MMKF formulation dominates across all performance metrics, and the preferred filter may depend strongly on the operational context. In precision-oriented tracking applications, such as collision avoidance, cooperative formation control, or guidance support, minimizing state estimation error is typically the primary objective. In these scenarios, a formulation yielding the lowest RMSE may be preferred, even if it exhibits relatively frequent mode switching or moderate instability in model identification.

Conversely, in surveillance, intent inference, or threat assessment tasks, stable and reliable identification of the underlying motion regime may be more critical than marginal improvements in estimation accuracy. Excessive mode switching, reflected by low dwell times, may lead to spurious maneuver detections or unstable higher-level decision logic. In such cases, a filter that provides longer dwell times and more consistent model classification, despite slightly higher RMSE, may be operationally advantageous.

Similarly, confusion matrix analysis becomes particularly relevant when different motion models trigger distinct supervisory or control actions. Accurate discrimination between coordinated turns, accelerations, or steady flight may therefore outweigh small differences in position or velocity error.

5. Conclusions

In this paper, four MMKF formulations for UAV tracking—GPB1, IMM, χ^2 -test-based, and *t*-test-based—are presented and compared. The analysis emphasizes the role of the transition probability matrix, which governs the likelihood of the target switching between motion modes, and its impact on both estimation accuracy and mode identification. In

addition to RMSE, metrics such as confusion matrices and dwell times are introduced to capture performance nuances in model selection accuracy and filter stability. Through such a joint analysis, this work provides practical guidance for selecting MMKF formulations according to mission-specific requirements rather than relying on a single scalar performance indicator. Future research will extend the simulation scenario to a 3D environment and to more complex motion models. Moreover, future works may explore hybrid strategies that combine the strengths of these approaches or leverage reinforcement learning to adaptively optimize TPM parameters in real time, enhancing tracking robustness in highly maneuvering UAV scenarios.

Author Contributions: Conceptualization, F.F.L. and E.I.T.; methodology, F.F.L. and E.I.T.; software, F.F.L.; validation, F.F.L. and E.I.T.; formal analysis, F.F.L., E.I.T., E.C. and Y.F.; investigation, F.F.L., E.I.T., E.C. and Y.F.; resources, F.F.L. and E.I.T.; data curation, F.F.L. and E.I.T.; writing—original draft preparation, F.F.L. and E.I.T.; writing—review and editing, F.F.L., E.I.T., E.C. and Y.F.; visualization, F.F.L. and E.I.T.; supervision, F.F.L., E.C. and Y.F.; project administration, E.C. and Y.F.; funding acquisition, E.C. and Y.F. All authors have read and agreed to the published version of the manuscript.

Funding: This research received no external funding.

Institutional Review Board Statement: Not applicable.

Informed Consent Statement: Not applicable.

Data Availability Statement: The raw data supporting the conclusions of this article will be made available by the authors on request.

Conflicts of Interest: The authors declare no conflicts of interest.

Abbreviations

The following abbreviations are used in this manuscript:

CA	Constant Acceleration
CT	Constant Turn rate
CV	Constant Velocity
GPB	Generalized Pseudo Bayesian
IMM	Interacting Multiple Models
MMKF	Multiple-Model Kalman Filter
RMSE	Root Mean Square Error
TPM	Transition Probability Matrix
UAV	Unmanned Aerial Vehicle

References

1. Stanković, S.S.; Stanković, M.S.; Stipanović, D.M. Consensus-based Overlapping Decentralized Estimation with Missing Observations and Communication Faults. *Automatica* **2009**, *45*, 1397–1406. [[CrossRef](#)]
2. Khodarahmi, M.; Maihami, V. A Review on Kalman Filter Models. *Arch. Comput. Methods Eng.* **2022**, *30*, 727–747. [[CrossRef](#)]
3. Olfati-Saber, R.; Shamma, J. Consensus Filters for Sensor Networks and Distributed Sensor Fusion. In *Proceedings of the 44th IEEE Conference on Decision and Control*; IEEE: Piscataway, NJ, USA, 2005; pp. 6698–6703. [[CrossRef](#)]
4. Olfati-Saber, R. Distributed Kalman filtering for Sensor Networks. In *Proceedings of the 2007 46th IEEE Conference on Decision and Control*; IEEE: Piscataway, NJ, USA, 2007; pp. 5492–5498. [[CrossRef](#)]
5. Ding, Z.; Liu, Y.; Liu, J.; Yu, K.; You, Y.; Jing, P.; He, Y. Adaptive Interacting Multiple Model Algorithm Based on Information-Weighted Consensus for Maneuvering Target Tracking. *Sensors* **2018**, *18*, 2012. [[CrossRef](#)] [[PubMed](#)]
6. Lizzio, F.F.; Bugaj, M.; Rostáš, J.; Primates, S. Comparison of Multiple Models in Decentralized Target Estimation by a UAV Swarm. *Drones* **2024**, *8*, 5. [[CrossRef](#)]
7. Fantacci, C.; Battistelli, G.; Chisci, L.; Farina, A.; Graziano, A. Multiple-model algorithms for Distributed Tracking of a Maneuvering Target. In *15th International Conference on Information Fusion, FUSION 2012*; IEEE: Piscataway, NJ, USA, 2012; pp. 1028–1035.

8. Chisci, L.; Fantacci, C.; Graziano, A.; Farina, A.; Battistelli, G. Consensus-based Multiple-model Bayesian Filtering for Distributed Tracking. *IET Radar Sonar Navig.* **2014**, *9*, 401–410. [[CrossRef](#)]
9. Li, X.R.; Jilkov, V.P. Survey of maneuvering target tracking. Part V: Multiple-model methods. *IEEE Trans. Aerosp. Electron. Syst.* **2005**, *41*, 1255–1321. [[CrossRef](#)]
10. Anderson, T.; Goodman, L. Statistical Inference About Markov Chains. *Ann. Math. Stat.* **1957**, *28*, 89–110. [[CrossRef](#)]
11. Du, M.; Bi, D.; Wang, S. The Interacting Multiple Model Algorithm based on Adaptive Markov Transition Probability. In *Proceedings of the 2017 IEEE International Conference on Signal Processing, Communications and Computing (ICSPCC)*; IEEE: Piscataway, NJ, USA, 2017; pp. 1–6. [[CrossRef](#)]
12. Lee, I.; Park, C. An Improved Interacting Multiple Model Algorithm With Adaptive Transition Probability Matrix Based on the Situation. *Int. J. Control Autom. Syst.* **2023**, *21*, 3299–3312. [[CrossRef](#)]
13. Cosme, L.B.; D'Angelo, M.F.S.V.; Caminhas, W.M.; Camargos, M.O.; Palhares, R.M. An Adaptive Approach for Estimation of Transition Probability Matrix in the Interacting Multiple Model Filter. *J. Intell. Fuzzy Syst.* **2021**, *41*, 155–166. [[CrossRef](#)]
14. Wolfe, S.; Givigi, S.; Rabbath, C.A. Multiple Model Distributed EKF for Teams of Target Tracking UAVs using T Test Selection. *J. Intell. Robot. Syst.* **2022**, *104*, 56. [[CrossRef](#)]
15. Li, X.; Jilkov, V. Survey of Maneuvering Target Tracking. Part I: Dynamic Models. *IEEE Trans. Aerosp. Electron. Syst.* **2003**, *39*, 1333–1364. [[CrossRef](#)]
16. Schubert, R.; Richter, E.; Wanielik, G. Comparison and evaluation of advanced motion models for vehicle tracking. In *Proceedings of the 2008 11th International Conference on Information Fusion*; IEEE: Piscataway, NJ, USA, 2008; pp. 1–6.
17. Wells, J.Z.; Kumar, R.; Kumar, M. Application of Interacting Multiple Model for Future State Prediction of Small Unmanned Aerial Systems. In *Proceedings of the 2021 American Control Conference (ACC)*; IEEE: Piscataway, NJ, USA, 2021; pp. 3755–3760. [[CrossRef](#)]
18. Noack, B.; Sijs, J.; Hanebeck, U.D. Fusion Strategies for Unequal State Vectors in Distributed Kalman Filtering. *IFAC Proc. Vol.* **2014**, *47*, 3262–3267. [[CrossRef](#)]
19. Li, W.; Jia, Y. An information theoretic approach to interacting multiple model estimation. *IEEE Trans. Aerosp. Electron. Syst.* **2015**, *51*, 1811–1825. [[CrossRef](#)]
20. Granström, K.; Willett, P.; Bar-Shalom, Y. Systematic Approach to IMM mixing for Unequal Dimension States. *IEEE Trans. Aerosp. Electron. Syst.* **2015**, *51*, 2975–2986. [[CrossRef](#)]

Disclaimer/Publisher's Note: The statements, opinions and data contained in all publications are solely those of the individual author(s) and contributor(s) and not of MDPI and/or the editor(s). MDPI and/or the editor(s) disclaim responsibility for any injury to people or property resulting from any ideas, methods, instructions or products referred to in the content.